ACS Macro Letters

Letter

Cite This: ACS Macro Lett. 2018, 7, 184−189

pubs.acs.org/macroletters

Semiconductor Quantum Dots as Photocatalysts for Controlled Light-Mediated Radical Polymerization

Yiming Huang,[†,‡] Yifan Zhu,[†,‡] and Eilaf Egap*[,‡,§]

[‡]Department of Materials Science and NanoEngineering and [§]Department of Chemical and Biomolecular Engineering, Rice University, Houston, Texas 77005, United States

Supporting Information

ABSTRACT: Light-mediated radical polymerization has benefited from the rapid development of photoredox catalysts and offers many exceptional advantages over traditional thermal polymerizations. Nevertheless, the majority of the work relies on molecular photoredox catalysts or expensive transition metals. We exploited the capability of semiconductor quantum dots (QD) as a new type of catalyst for the radical polymerization that can harness natural sunlight. Polymerizations of (meth)acrylates, styrene, and construction of block copolymers were demonstrated, together with temporal control of the polymerization by the light source. Photoluminescence experiments revealed that the reduction of alkyl bromide initiator by photoexcited QD is the key to this light-mediated radical polymerization.

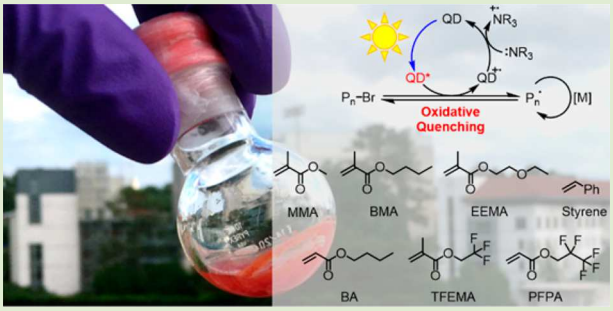

The design of functional polymers with well-defined structure and architecture and with the ability to precisely control the sequence, molecular weight, and molecular weight distribution has been of significant technological and fundamental interest. Atom transfer radical polymerization (ATRP)[1−3] has emerged as one of the most powerful polymerization methods for synthetic polymers with high precisions of chemical composition, length distribution, and complex architectures.[1−3] Recently, light-mediated ATRP has gained significant prominence as a strategy in enabling both spatial and temporal control over reaction kinetics and in regulating the activation and deactivations steps via external stimulus.[4,5] Furthermore, the ability to harness solar energy for chemical transformations using visible-light presents unique opportunities in using mild conditions and toward sustainability.[6] While initial reports of photomediated ATRP[7−10] and reversible addition−fragmentation chain-transfer (RAFT) polymerizations[5,11,12] have mostly focused on using precious transition-metal complexes (i.e., Ru(II) and Ir(III)), metal-free organic catalysts have also proven to be effective in light-mediated photopolymerizations.[13−18] However, most of the photomediated methodologies of polymerizations utilize traditional and nonfunctional monomers such as styrene and simple (methyl)acrylate derivatives and require extensive synthetic efforts and purification steps of the photocatalysts. Thus, in order to propel light-mediated polymerizations to the forefront, there is a need to explore varies strategies that are compatible with wide selections of functional monomers while also maintain simplicity, rapid synthesis, and purification of the photocatalysts.

Semiconductor quantum dots (QD), solution-dispersible nanocrystals, represent a promising class of photocatalysts for light-mediated controlled polymerizations. Unlike transition-metal complexes or organic photocatalysts, QD have strong and easily tunable absorption in the UV and visible range with large extinction coefficients ($\varepsilon > 10^5$ M^{-1} cm^{-1}),[19] large specific surface area that allows for binding of multiple substrates and, thus, may accelerate the rate of charge transfer,[20] and inherently high photostability compared to organic-based photocatalysts.[21,22] More importantly, QD photocatalysts can easily be synthesized and purified starting from inexpensive raw materials, with the ability to easily fine-tune size dimensions, shape, and ligands with the goal of tuning redox potentials,[23] absorption spectra, or even interactions with synthetic substrates to allow for wide selections of functional monomers. Indeed, recent reports by Weiss, Weix, and co-workers have independently demonstrated QD as excellent photocatalysts in the synthesis of small molecules, primary in C−C coupling, amine arylation, and reductive dehalogenation.[20,24] Early efforts for radical polymerization of (meth)acrylate monomers using nanocrystalline semiconductors (ZnO and TiO_2) as the photocatalyst were very limited and suffered from poor control of molecular weight distributions and low monomer conversion.[25−28] Furthermore, photoexcitation of these high bandgap semiconductors requires shortwave UV irradiation, which only contributes to a small fraction of solar irradiation.[29−31] Subsequent examples of light-initiated polymerization of acrylate-based monomers using either CdS or CdTe were reported.[32−34] Detailed mechanistic studies

Received: December 13, 2017
Accepted: January 19, 2018
Published: January 24, 2018

DOI: 10.1021/acsmacrolett.7b00968
ACS Macro Lett. 2018, 7, 184−189

suggested that surface modifications of CdS by amines played an important role in improving the initiation efficiency.[32,33] These QD-catalyzed polymerizations were not living-type polymerizations and could not be classified as ATRP.

Herein, we report controlled photomediated ATRP facilitated by QD as the versatile photoredox catalyst (Figure 1). We

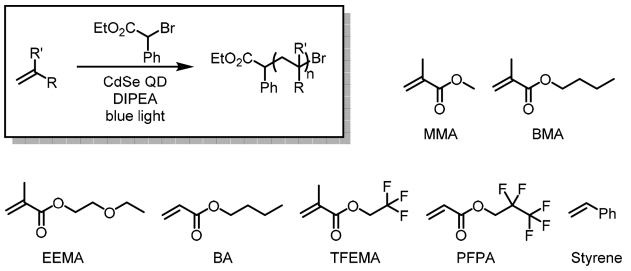

Figure 1. Controlled radical polymerization driven by blue LED light (10 mW/cm^2) at 25 °C in the presence of CdSe QD as the photocatalyst.

establish a broad scope of functional monomers under irradiation of visible light sources such as natural sunlight and household lamps. Our kinetic studies under both continuous and intermittent light exposure demonstrate control over the polymerization progress by light. Meanwhile, chain extension reactions of isolated polymers indicate the "living" nature of the radical polymerization.

We envisioned that the unique electronic and photophysical properties of QD would allow for highly responsive photo controlled living radical polymerization. We anticipated that upon photoexcitation of QD, the photoexcited QD* would reduce the alkyl bromide initiator to give the desired alkyl radical, which would subsequently initiate the polymerization of acrylate monomers. A key requirement is that the reduction potential of QD* should be sufficiently reducing to activate alkyl radical initiators. Among common alkyl bromide initiators used in ATRP, ethyl α-bromophenylacetate (EBP) is known to have the highest initiation efficiency,[15] and therefore was used as the initiator in this work. We examined cadmium selenide (CdSe) QD as a photocatalyst for ATRP. The size and dimensions of CdSe nanocrystals can easily be varied in order to tune the excitonic absorption peak spanning the entire visible spectrum.[34] Given that both the absorption spectra and reduction potential are influenced by the size of QD nanocrystals,[20] we chose to synthesize medium-size CdSe nanocrystals with an estimated diameter of 3.3 nm, correlating to an absorption peak of 565 nm (ε = 1.35 × 10^5 M^{-1} cm^{-1}),[35] and a reduction potential of excited CdSe QD* of −1.59 V versus SCE.[20] This reduction potential of 3.3 nm CdSe QD* is sufficiently negative to activate the EBP initiator (EBP/EBP$^{\bullet-}$ E = −0.74 V vs SCE).[20] A molar concentration of 0.4 mM CdSe QD dispersion was used in all of the reactions corresponding to a catalyst loading of 0.6 mol % with respect to the monomer concentration.

We initially examined CdSe QD as the photocatalyst in the polymerization of methyl methacrylate (MMA), EBP as the initiator, in the presence of excess *N*,*N*-diisopropylethylamine (DIPEA) in tetrahydrofuran (THF) with a household blue LED (460−480 nm) light source (Figure 1). The reaction generated PMMA in 69.5% isolated yield in 16 h with a number-average molecular weight (M_n) of 41.7 kDa, and a polydispersity ($Đ$) of 1.67 (Table 1, entry 1). While an excess

Table 1. Results of the Living Radical Polymerizations Using CdSe QD as a Photoredox Catalyst[a]

entry	monomer	[DIPEA]/[mono]	solv.	conv[b] (%)	M_n[c] (kDa)	$Đ$[d]
1	MMA	2	THF	68.5[e]	41.5	1.67
2	MMA	0.05	THF	48.3[e]	40.4	1.68
3	MMA	0.05	DMF	76.3	26.0	1.38
4	MMA	0.05	C_6H_6	92.8	23.6	1.68
5[f]	MMA	0.05	C_6H_6	83.6	38.3	1.37
6	BMA	1	neat	82.6	47.7	1.38
7	BA	0.05	C_6H_6	81.8	33.3	1.68
8	EEMA	1	neat	99.0	36.1	1.82
9	TFEMA	0.2	neat	76.0	30.3	1.39
10	PFPA	0.05	C_6H_6	68.2	10.6	1.25
11	Styrene	0.2	neat	35.7	9.69	1.62

[a]Notes: Polymerizations carried out in the deaerated environment at ambient temperature and were irradiated with a 10 W household blue LED lamp (460−480 nm) for 16 h. [b]Monomer conversion determined by ^{1}H NMR spectrum of the reaction liquor. [c]Number-average (M_n) and weight-average (M_w) molecular weights were determined by gel permeation chromatography (GPC). [d]Polydispersity index defined as $Đ$ = M_w/M_n. [e]Isolated polymer product by precipitation in MeOH. [f]Under natural sunlight for 8 h.

of trialkylamine is often necessary for the photoredox synthesis of small molecules,[20,24] it can also promote undesired side reactions that consume the radical species.[36] To circumvent side reactions, we decreased the concentration of amines (Table 1, entry 2) and found that 0.05 equiv DIPEA (to monomer) is sufficient to achieve comparable conversion and polydispersity to that of excess amine. Varies initiators were examined including diethyl 2-bromo-2-methylmalonate (DBMM) and ethyl α-bromoisobutyrate (EBiB). Among the three initiators we studied, EBP resulted in higher MMA conversion and better controlled polymer chain growth (Table S1, entries 13, 16, and 17), and it was therefore used in subsequent polymerizations. To benchmark the polymerization efficiency facilitated by QD, we carried out the same polymerization with commercially available dyes such as perylene and fluorescein (Table S1, entries 13−15).[15,37] In similar reaction conditions, QD consistently resulted in a higher MMA conversion and narrower (or comparable) polydispersity.

The effect of solvent polarity on the polymerization was further probed (Figure 1). Polar solvents are typically the primary choice for many reported photoredox associated ATRP,[13,15] and are known to stabilize charge-separated species.[15] In general, an increase in the conversion is observed with less polar solvents, while a decrease in the polydispersity is observed with high polar solvents. For example, when DMF was used as a solvent, a conversion of 76.3% of MMA and $Đ$ of 1.37 was obtained (Table 1, entry 3), compared to a conversion of 92.8% and $Đ$ of 1.86 when using benzene as a solvent (Table 1, entry 4). Attempts to use high dielectric solvents (DMSO, MeOH) were unsuccessful in yielding any polymers and resulted in significant aggregations of the QD. To minimize degradation, the QD was capped with a protective layer of alkylated ligands (oleic acid and trioctylphosphine) which are incompatible with very polar solvents. Our ongoing research aims to address this issue by exploring polar ligands. Interestingly, the use of solar irradiation resulted in a low polydispersity (Table 1, entry 5) as reported in the literature.[15] We systematically then varied the power output of the blue LED from 2.5, to 5.6 and 10 mW/cm^2 to probe the observed

DOI: 10.1021/acsmacrolett.7b00968
ACS Macro Lett. 2018, 7, 184−189

enhanced percent conversion and polydispersity. In general, higher light intensity resulted in higher MMA conversion and narrow polydisersity (Table S1, entries 19−21). This suggest that higher power output results in enhanced rate of initiation.

We sought to evaluate the generality and compatibility of QD as a photocatalyst with various functional monomers given their excellent performance with MMA. Polymers of butyl methacrylate (BMA) and butyl acrylate (BA) were synthesized using similar conditions to that of MMA. The neat polymerization of BMA resulted in a conversion of 82.6% with a low $Đ$ of 1.37, while polymerization of BA in benzene gave a conversion of 81.8% and $Đ$ of 1.68 (Table 1, entries 6 and 7). Polymers with functional monomers such as 2-ethoxy ethyl methacrylate (EEMA) are important in biomedical applications and can be effective for oxygen transport.[38] Polymerization of EEMA resulted in a high conversion of 99% and $Đ$ 1.82. The absence of photocatalysts or initiator, reactions did not yield any polymers (Table S2, entries 18 and 19). This suggest that the large $Đ$ is due to high monomer conversion and chain combination toward the end of polymerization.

An important class of functional polymers includes fluorinated and semifluorinated polymers due to their low refractive index and hydrophobic properties that result in intriguing characteristics and broad applications.[39,40] We demonstrate highly effective and controlled polymerization of 2,2,2-trifluoroethyl methacrylate (TFEMA) and 2,2,3,3,3-pentafluoropropyl acrylate (PFPA) with our protocol that results in fluorinated polymers with high conversion of 76.0% and 68.2%, and low $Đ$ of 1.39 and 1.25, respectively (Table 1, entries 9 and 10). Polymerization of most monomers in neat conditions is possible and a conversion of up to 75% can be reached, while still retaining a moderately narrow mass distribution ($Đ$ = 1.2−1.8). Polymerization of styrene using photomediated conditions was previously reported to be a challenge due to the relatively low reactivity of styrene monomer compared to most (meth)acrylate monomers.[14,41] We addressed this problem by carrying out the polymerization in a solvent-free environment and obtained polystyrene (PS) with a 35.7% conversion and a $Đ$ of 1.62 (entry 11).

To elucidate the mechanism of the photoredox catalyzed polymerization of MMA, we performed a range of control experiments. The absence of either the QD, DIPEA, or light irradiation did not result in polymer formation, demonstrating a photomediated polymerization that is catalyzed by QD. To further prove the necessity of light irradiation, the progress of polymerization was probed under continuous and intermittent light conditions and MMA conversion was monitored at each time interval (Figure 2a). Irradiation of the monomer, initiator, and QD mixture with a blue LED for 2 h at room temperature resulted in 16% monomer conversion. Removal of the light source for 1 h in the darkness stops the polymerization and results in no monomer conversion. These turn "on/off" cycles can be repeated several times, in which the MMA conversion increases only during the light irradiation cycle and halts completely in the darkness. A plot of $\ln([M]_0/[M]_t)$ versus total exposure time follows a linear relationship and a first-order kinetics (Figure 2b). The data proves that in the absence of light, the polymerization stops and activation of the chain ends is not occurring. Analogous to conventional ATRP, the photoredox process activates the polymer chains as propagating radicals, which in the dark return to dormant alkyl bromide species.[13] These results demonstrate a high degree of temporal control and evidence of photocontrolled living radical polymerization promoted by QD as a photocatalyst for reversible activation/deactivation of Br chain end.

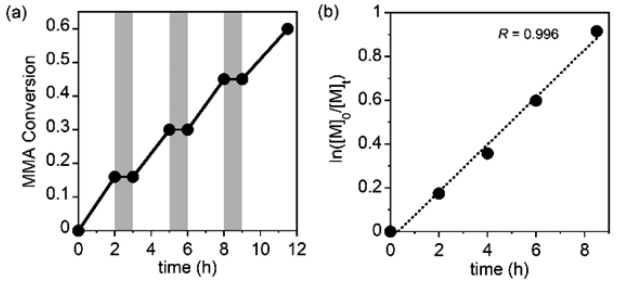

Figure 2. (a) MMA conversion monitored vs reaction time under periodic switching blue light irradiation (white regions) and darkness (shaded regions). (b) First order kinetic profile of monomer concentration vs time under continuous light irradiation.

A fundamental factor in a successful synthesis of diverse and functional macromolecules with well-defined architectures relies on high chain-end fidelity in controlled radical polymerizations such as ATRP. To verify the livingness of the resultant polymers, a series of block copolymers were prepared using sequential photocontrolled living radical polymerization (Figures 3 and S2). PS, PMMA and PTFEMA were used as

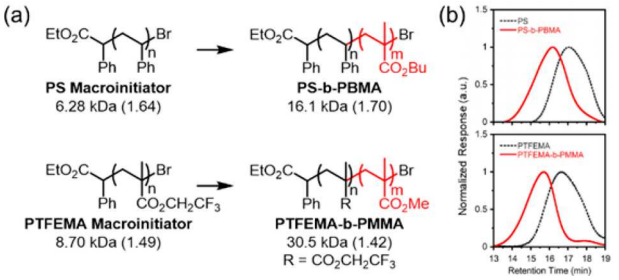

Figure 3. (a) Molecular structures of macroinitiators (PS and PTFEMA), block copolymers (PS-*b*-PBMA and PTFEMA-*b*-PMMA), and their respective M_n and $Đ$. (b) GPC traces of the corresponding macroinitiators and the block copolymers.

the macroinitiator in the polymerization of various monomers including MMA, TFEMA, and BMA to make the corresponding block copolymers (PS-*b*-PBMA, PS-*b*-PMMA, PS-*b*-PTFEMA, PTFEMA-*b*-PMMA, and PMMA-*b*-PTFEMA). The macroinitiators were first isolated, purified and then reintroduced to polymerization conditions to make each block copolymers. Successful chain extension and further polymerization were evidenced by GPC and ^{1}H NMR, providing high molecular weight and diverse block copolymers. GPC analysis showed a decrease in the retention time of chain extension products compared to that of the original macroinitiator (Figures 3b and S2), correlating to a substantial increase in the M_n. Furthermore, ^{1}H NMR analysis confirmed the degree of control in the macromolecular composition and incorporation of the monomers that formed the new block copolymers (Figures S6−S10). For example, in the case of PS-*b*-PTFEMA where the resonance peaks at 6.3−7.2 ppm correspond to the phenyl rings in PS, several new peaks appeared including the 4.31 ppm of the methylene group ($-C\mathbf{H}_2CF_3$) that correspond to protons resonance in PTFEMA. According to peak integrations, a molar ratio of styrene/TFEMA of 1:0.25 was determined with an estimated M_n of 8.80 kDa and $Đ$ = 1.31 of the final block copolymers, which is in good agreement with the

DOI: 10.1021/acsmacrolett.7b00968
ACS Macro Lett. 2018, 7, 184−189

GPC analysis (9.40 kDa; Table S2). In general, the PMMA and PTFEMA are more efficient in chain extension with a significant increase in M_n (17−21 kDa) than the PS macroinitiator (<10 kDa). These results suggest that the isolated polymer consists of Br-terminated polymer chain which was able to reinitiate the polymerization. It is likely caused by the reversible chain termination, an important feature in ATRP process, and such polymer chain with alkyl bromide terminal can be considered a "living" chain. It is possible that some homopolymer chains may not have the desired Br terminal due to radical chain combination or disproportionation, as we observed moderate overlap in GPC traces of macroinitiators and copolymers.[15]

To further probe the mechanism and redox processes in this living radical polymerization, we considered two possible and similar mechanisms and examined the role of the DIPEA (Figure S4). Both mechanisms start with the photoexcitation of the QD to generate the excited state QD* which subsequently reduce the dormant alkyl bromide chain to a radical, and a reversible termination of the propagating radical chain. A major difference between the two proposed mechanisms is the quenching pathway of QD*. The QD* can play a role as a strong oxidant or a reductant. In the oxidative pathway (Figure 4b), a single electron transfer (SET) takes place as QD*

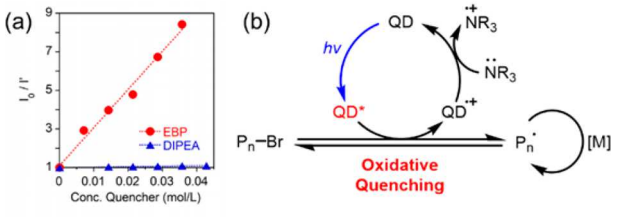

Figure 4. (a) Stern−Volmer plot of QD fluorescence (λ_{ex} = 460 nm) effectively quenched by EBP but not by DIPEA. (b) Proposed mechanisms of a photoinitiated polymerization catalyzed by CdSe QD. Each intersection between arrows indicates a single electron transfer (SET) event.

donates an electron to the alkyl bromide and forms a radical cation ($QD^{\bullet+}$). On the other hand, QD* can also accept an electron from the trialkylamine (NR_3) and become a QD radical anion ($QD^{\bullet-}$) in the reductive pathway (Figure S4).[16] Through SET process with QD*, the alkyl bromide (P_n−Br) or the trialkylamine (NR_3) is a potential QD* fluorescence quencher in each pathway. While most ATRP photoredox catalysts proceed through an oxidative pathway without an electron donor,[13−15] amines often act as an important sacrificial electron donor in catalytic photoredox reactions.[41] However, in this polymerization method, DIPEA as little as 0.05 equiv of MMA proved to be sufficient to produce conversion of >90%. To identify the dominant SET pathway in this polymerization, we used the Stern−Volmer relationship to evaluate the change in the QD* photoluminescence (PL) at various concentrations of EBP or DIPEA (Figure 4a). The Stern−Volmer plot shows a linear relationship in the ratio of I_0/I' PL intensity (I_0 = PL intensity in the absence of quencher, and I' = PL intensity with a given concentration of a quencher) as an increase in EBP concentration, indicative of CdSe fluorescence quenching by EBP. In contrast, DIPEA was far less effective in quenching CdSe fluorescence (Figure S3), contrary to previous reports that showed strong quenching effect by trialkylamine.[20] These results and the redox potentials (Figure S5) suggest that the excited state of CdSe is more likely undergoing a redox process with EBP and not with the DIPEA, and therefore, an oxidative quenching pathway could be the major contribution in this radical polymerization. We note that the polymerization proceeds in the absence of the EBP as previously reported.[32,33]

In that case, there are other possible mechanisms, either a ligand exchange with amines facilitates radical generation on the QD surface, followed by direct radical transfer to MMA monomer, as suggested previously,[32] or DIPEA radical cation, formed as result of electron transfer to QD, initiates the radical polymerization. We think the later mechanism is unlikely based on fluorescence studies (Figures 4a and S3) and redox potentials (Figure S5). In both cases, the polymerization is better classified as photoinitiated rather than photocontrolled polymerization.

In conclusion, we have demonstrated that semiconductor CdSe QD are effective photoredox catalysts for photocontrolled living radical polymerization. Light-mediated ATRP facilitated by QD achieved similar or superior performance in a scope of a wide variety of functional acrylate monomers and controlled polymerization with high conversion and narrow polydispersity to that of organic or metal complex photocatalysts. Through studies of macroinitiator chain extension and reaction progress under intermittent light exposure, the photomediated ATRP exhibited spatial and temporal control of the polymer architectures. We envision that advantages such as facile synthetic and purification preparation, low catalyst loading combined with the ability to easily tune redox and electronic properties will result in a broader application of QD as a photocatalyst for various types of polymerization. Future work will focus on variations of QD surface chemistry, ligand exchange and elemental compositions to achieve higher initiation efficiency and further control of molecular weights and distributions.

■ ASSOCIATED CONTENT

Supporting Information

The Supporting Information is available free of charge on the ACS Publications website at DOI: 10.1021/acsmacrolett.7b00968.

Experimental procedures, Figures S1−S10, and Tables S1−S4 (PDF).

■ AUTHOR INFORMATION

Corresponding Author

*E-mail: ee30@rice.edu.

ORCID

Eilaf Egap: 0000-0002-6106-5276

Author Contributions

†These authors contributed equally.

Notes

The authors declare no competing financial interest.

■ ACKNOWLEDGMENTS

This work was supported in part by NSF Grant CHE-1710225 (E.E.). The authors acknowledge the use of instrumentation and help from Dr. Christopher Pennington at Rice Mass Spectrometry Facility. We thank Professor Tim Lian and Mr. Zihao Xu for guidance with the synthesis of CdSe QD and insightful discussions.

DOI: 10.1021/acsmacrolett.7b00968
ACS Macro Lett. 2018, 7, 184−189

REFERENCES

(1) Wang, J.-S.; Matyjaszewski, K. Controlled/"living" radical Polymerization. Atom Transfer Radical Polymerization in the Presence of Transition-Metal Complexes. *J. Am. Chem. Soc.* **1995**, *117* (20), 5614−5615.

(2) Matyjaszewski, K.; Xia, J. Atom Transfer Radical Polymerization. *Chem. Rev.* **2001**, *101* (9), 2921−2990.

(3) Matyjaszewski, K.; Tsarevsky, N. V. Macromolecular Engineering by Atom Transfer Radical Polymerization. *J. Am. Chem. Soc.* **2014**, *136* (18), 6513−6533.

(4) Chen, M.; Zhong, M.; Johnson, J. A. Light-Controlled Radical Polymerization: Mechanisms, Methods, and Applications. *Chem. Rev.* **2016**, *116* (17), 10167−10211.

(5) Corrigan, N.; Shanmugam, S.; Xu, J.; Boyer, C. Photocatalysis in Organic and Polymer Synthesis. *Chem. Soc. Rev.* **2016**, *45* (22), 6165−6212.

(6) Schultz, D. M.; Yoon, T. P. Solar Synthesis: Prospects in Visible Light Photocatalysis. *Science (Washington, DC, U. S.)* **2014**, *343* (6174), 1239176.

(7) Fors, B. P.; Hawker, C. J. Control of a Living Radical Polymerization of Methacrylates by Light. *Angew. Chem., Int. Ed.* **2012**, *51* (35), 8850−8853.

(8) Konkolewicz, D.; Schröder, K.; Buback, J.; Bernhard, S.; Matyjaszewski, K. Visible Light and Sunlight Photoinduced ATRP with Ppm of Cu Catalyst. *ACS Macro Lett.* **2012**, *1* (10), 1219−1223.

(9) Anastasaki, A.; Nikolaou, V.; Zhang, Q.; Burns, J.; Samanta, S. R.; Waldron, C.; Haddleton, A. J.; McHale, R.; Fox, D.; Percec, V.; et al. Copper(II)/Tertiary Amine Synergy in Photoinduced Living Radical Polymerization: Accelerated Synthesis of ω-Functional and A,ω-Heterofunctional Poly(acrylates). *J. Am. Chem. Soc.* **2014**, *136* (3), 1141−1149.

(10) Alfredo, N. V.; Jalapa, N. E.; Morales, S. L.; Ryabov, A. D.; Le Lagadec, R.; Alexandrova, L. Light-Driven Living/Controlled Radical Polymerization of Hydrophobic Monomers Catalyzed by Ruthenium-(II) Metalacycles. *Macromolecules* **2012**, *45* (20), 8135−8146.

(11) Xu, J.; Jung, K.; Atme, A.; Shanmugam, S.; Boyer, C. A Robust and Versatile Photoinduced Living Polymerization of Conjugated and Unconjugated Monomers and Its Oxygen Tolerance. *J. Am. Chem. Soc.* **2014**, *136* (14), 5508−5519.

(12) Xu, J.; Shanmugam, S.; Duong, H. T.; Boyer, C. Organo-Photocatalysts for Photoinduced Electron Transfer-Reversible Addition−fragmentation Chain Transfer (PET-RAFT) Polymerization. *Polym. Chem.* **2015**, *6* (31), 5615−5624.

(13) Treat, N. J.; Sprafke, H.; Kramer, J. W.; Clark, P. G.; Barton, B. E.; Read de Alaniz, J.; Fors, B. P.; Hawker, C. J. Metal-Free Atom Transfer Radical Polymerization. *J. Am. Chem. Soc.* **2014**, *136* (45), 16096−16101.

(14) Theriot, J. C.; Lim, C.-H.; Yang, H.; Ryan, M. D.; Musgrave, C. B.; Miyake, G. M. Organocatalyzed Atom Transfer Radical Polymerization Driven by Visible Light. *Science (Washington, DC, U. S.)* **2016**, *352* (6289), 1082−1086.

(15) Miyake, G. M.; Theriot, J. C. Perylene as an Organic Photocatalyst for the Radical Polymerization of Functionalized Vinyl Monomers through Oxidative Quenching with Alkyl Bromides and Visible Light. *Macromolecules* **2014**, *47* (23), 8255−8261.

(16) Lim, C.-H.; Ryan, M. D.; McCarthy, B. G.; Theriot, J. C.; Sartor, S. M.; Damrauer, N. H.; Musgrave, C. B.; Miyake, G. M. Intramolecular Charge Transfer and Ion Pairing in *N,N* -Diaryl Dihydrophenazine Photoredox Catalysts for Efficient Organocatalyzed Atom Transfer Radical Polymerization. *J. Am. Chem. Soc.* **2017**, *139* (1), 348−355.

(17) Huang, Z.; Gu, Y.; Liu, X.; Zhang, L.; Cheng, Z.; Zhu, X. Metal-Free Atom Transfer Radical Polymerization of Methyl Methacrylate with Ppm Level of Organic Photocatalyst. *Macromol. Rapid Commun.* **2017**, *38* (10), 1600461.

(18) Discekici, E. H.; Treat, N. J.; Poelma, S. O.; Mattson, K. M.; Hudson, Z. M.; Luo, Y.; Hawker, C. J.; de Alaniz, J. R. A Highly Reducing Metal-Free Photoredox Catalyst: Design and Application in Radical Dehalogenations. *Chem. Commun.* **2015**, *51* (58), 11705−11708.

(19) Smith, A. M.; Nie, S. Semiconductor Nanocrystals: Structure, Properties, and Band Gap Engineering. *Acc. Chem. Res.* **2010**, *43* (2), 190−200.

(20) Caputo, J. A.; Frenette, L. C.; Zhao, N.; Sowers, K. L.; Krauss, T. D.; Weix, D. J. General and Efficient C−C Bond Forming Photoredox Catalysis with Semiconductor Quantum Dots. *J. Am. Chem. Soc.* **2017**, *139* (12), 4250−4253.

(21) Chan, W. C.; Nie, S. Quantum Dot Bioconjugates for Ultrasensitive Nonisotopic Detection. *Science* **1998**, *281* (5385), 2016−2018.

(22) Jaiswal, J. K.; Mattoussi, H.; Mauro, J. M.; Simon, S. M. Long-Term Multiple Color Imaging of Live Cells Using Quantum Dot Bioconjugates. *Nat. Biotechnol.* **2003**, *21* (1), 47−51.

(23) Burda, C.; Chen, X.; Narayanan, R.; El-Sayed, M. A. Chemistry and Properties of Nanocrystals of Different Shapes. *Chem. Rev.* **2005**, *105* (4), 1025−1102.

(24) Zhang, Z.; Edme, K.; Lian, S.; Weiss, E. A. Enhancing the Rate of Quantum-Dot-Photocatalyzed Carbon−Carbon Coupling by Tuning the Composition of the Dot's Ligand Shell. *J. Am. Chem. Soc.* **2017**, *139* (12), 4246−4249.

(25) Hoffman, A. J.; Yee, H.; Mills, G.; Hoffmann, M. R. Photoinitiated Polymerization of Methyl Methacrylate Using Q-Sized Zinc Oxide Colloids. *J. Phys. Chem.* **1992**, *96* (13), 5540−5546.

(26) Hoffman, A. J.; Mills, G.; Yee, H.; Hoffmann, M. R. Q-Sized Cadmium Sulfide: Synthesis, Characterization, and Efficiency of Photoinitiation of Polymerization of Several Vinylic Monomers. *J. Phys. Chem.* **1992**, *96* (13), 5546−5552.

(27) Stroyuk, A. L.; Granchak, V. M.; Korzhak, A. V.; Kuchmii, S. Y. Photoinitiation of Buthylmethacrylate Polymerization by Colloidal Semiconductor Nanoparticles. *J. Photochem. Photobiol., A* **2004**, *162* (2), 339−351.

(28) Ojah, R.; Dolui, S. K. Photopolymerization of Methyl Methacrylate Using Dye-Sensitized Semiconductor Based Photocatalyst. *J. Photochem. Photobiol., A* **2005**, *172* (2), 121−125.

(29) Ni, X.; Ye, J.; Dong, C. Kinetics Studies of Methyl Methacrylate Photopolymerization Initiated by Titanium Dioxide Semiconductor Nanoparticles. *J. Photochem. Photobiol., A* **2006**, *181* (1), 19−27.

(30) Dadashi-Silab, S.; Atilla Tasdelen, M.; Mohamed Asiri, A.; Bahadar Khan, S.; Yagci, Y. Photoinduced Atom Transfer Radical Polymerization Using Semiconductor Nanoparticles. *Macromol. Rapid Commun.* **2014**, *35* (4), 454−459.

(31) Wang, X.; Lu, Q.; Wang, X.; Joo, J.; Dahl, M.; Liu, B.; Gao, C.; Yin, Y. Photocatalytic Surface-Initiated Polymerization on TiO2 toward Well-Defined Composite Nanostructures. *ACS Appl. Mater. Interfaces* **2016**, *8* (1), 538−546.

(32) Strandwitz, N. C.; Khan, A.; Boettcher, S. W.; Mikhailovsky, A. A.; Hawker, C. J.; Nguyen, T.-Q.; Stucky, G. D. One- and Two-Photon Induced Polymerization of Methylmethacrylate Using Colloidal CdS Semiconductor Quantum Dots. *J. Am. Chem. Soc.* **2008**, *130* (26), 8280−8288.

(33) Barichard, A.; Galstian, T.; Israëli, Y. Physico-Chemical Role of CdSe/ZnS Quantum Dots in the Photo-Polymerization Process of Acrylate Composite Materials. *Phys. Chem. Chem. Phys.* **2012**, *14* (22), 8208−8216.

(34) Jasieniak, J.; Califano, M.; Watkins, S. E. Size-Dependent Valence and Conduction Band-Edge Energies of Semiconductor Nanocrystals. *ACS Nano* **2011**, *5* (7), 5888−5902.

(35) Yu, W. W.; Qu, L.; Guo, W.; Peng, X. Experimental Determination of the Extinction Coefficient of CdTe, CdSe, and CdS Nanocrystals. *Chem. Mater.* **2003**, *15* (14), 2854−2860.

(36) Furst, L.; Matsuura, B. S.; Narayanam, J. M. R.; Tucker, J. W.; Stephenson, C. R. J. Visible Light-Mediated Intermolecular C−H Functionalization of Electron-Rich Heterocycles with Malonates. *Org. Lett.* **2010**, *12* (13), 3104−3107.

(37) Liu, X.; Zhang, L.; Cheng, Z.; Zhu, X. Metal-Free Photoinduced Electron Transfer−atom Transfer Radical Polymerization (PET−

DOI: 10.1021/acsmacrolett.7b00968
ACS Macro Lett. 2018, 7, 184−189

ATRP) via a Visible Light Organic Photocatalyst. *Polym. Chem.* **2016**, *7* (3), 689−700.
(38) Tiemblo, P.; Laguna, M. F.; Garcia, F.; Garcia, J. M.; Riande, E.; Guzman, J. Gas Transport Properties of Poly(2-Ethoxyethyl Methacrylate-Co-2-Hydroxyethyl Methacrylamide). *Macromolecules* **2004**, *37* (11), 4156−4163.
(39) Xiong, D.; Liu, G.; Hong, L.; Duncan, E. J. S. Superamphiphobic Diblock Copolymer Coatings. *Chem. Mater.* **2011**, *23* (19), 4357−4366.
(40) Discekici, E. H.; Anastasaki, A.; Kaminker, R.; Willenbacher, J.; Truong, N. P.; Fleischmann, C.; Oschmann, B.; Lunn, D. J.; Read de Alaniz, J.; Davis, T. P.; et al. Light-Mediated Atom Transfer Radical Polymerization of Semi-Fluorinated (Meth)acrylates: Facile Access to Functional Materials. *J. Am. Chem. Soc.* **2017**, *139* (16), 5939−5945.
(41) Zhang, G.; Song, I. Y.; Ahn, K. H.; Park, T.; Choi, W. Free Radical Polymerization Initiated and Controlled by Visible Light Photocatalysis at Ambient Temperature. *Macromolecules* **2011**, *44* (19), 7594−7599.

DOI: 10.1021/acsmacrolett.7b00968
ACS Macro Lett. 2018, 7, 184−189